Effective pathway of charge transfer in DNA duplex

Seongjin Kim and Juyeon Yi
Department of Physics, Pusan National University, Busan 609-735, Korea

Sun-Yong Hwang
Department of Physics, Korea University, Seoul 136-713, Korea

(Received 23 May 2008; revised manuscript received 12 January 2009; published 30 March 2009)

We examine the most efficient route for charge propagation in DNA duplex. We find a direct path along one strand and a detour using the complementary strand compete with each other. Charge tends to take the path along the strand whose energy levels are close to its energy, and yet there exists a crossover length N_c so that for a transfer over a distance shorter than N_c the direct path is always advantageous. We obtain the analytic results for the behavior together with various decay types such as a constant decay, an exponential decay, and a crossover between them, whose validity is confirmed by the numerical calculation.

DOI: 10.1103/PhysRevB.79.125119 PACS number(s): 87.14.gk, 72.80.Le, 87.15.Pc

Ever since Eley and Spivey[1] proposed the DNA "π way," charge migration in DNA molecules has been extensively studied in biochemistry and molecular electronics.[2] A variety of charge motions and underlying mechanisms have been known in relation to the diverse length dependence of charge-transfer rate. When a charge transmits via a "forbidden" state (or the band-gap state), it tunnels through the gap with an exponential tail responsible for the transfer rate given by $k(N)=k_0 \exp(-\beta N)$ with N being the length of the molecular bridge.[3,4] The observed decay scale has a wide range depending on donor and sequence.[5] When a charge migrates via the molecule energy states, it spreads over a large distance and yields an almost length-independent resonance transfer.[6] Meanwhile, a long-range charge transfer can be realized also by multiple hoppings assisted by the coupling to a dissipative environment.[7]

Charge motions in DNA are understood to some extent and, yet, a complete picture is far to reach due to the system complexity. Besides, some issues remain untouched despite its fundamental importance such as *which path* charge would cleverly take for the most efficient transfer. As shown in Fig. 1(a), for a duplex that can be viewed as a railway track, there exist many routes from the donor to acceptor site. For instance, the charge can take the direct path along one strand but also the detour accompanied by the back and forth hopping between the strands.

The purpose of this work is to examine the efficient transfer route by considering the charge transmission probability for each path via the Green's function method.[8] First, we focus on the charge propagation along one strand in order to investigate its length dependence and the decay scales. The decay types are found various according to the charge-carrier energy but commonly display a natural tendency that a charge having an energy closer to the energy states of the strand can propagate over a long distance. With the help of the results, we consider the interstrand coupling and charge transmission via the possible paths depicted in Fig. 1(a). Our key results are summarized in Fig. 1(b) presenting the ratios between the transmission along the direct path and the detour path. When the incident charge energy is close to the energy states of the strand 1 (for our numerical parameters, the energy levels of the strand 1 and the strand 2 are populated near $E \cong -4.3$ eV and $E \cong -1.1$ eV, respectively), the direct path is naturally favorable for a long-range transfer. This behavior persists up to a certain energy value at which the decay scales of the two strands become comparable with each other. As the energy increases further toward the energy levels of the strand 2, charge propagation along the strand 2 decays slower than the strand 1. A simple-minded guess would be that the detour using the strand 2 is preferred, but it turns out that there exists a crossover distance N_c; charge transfer over a short distance $N<N_c$ still takes place mainly via the direct path. We determine N_c as a function of the energy analytically, in parallel check with numerical evaluations. Further we show that the competition between the two paths is responsible for the distance-dependence crossover observed in recent experiment.[9]

We begin with the tight-binding Hamiltonian for a homogeneously sequenced DNA duplex. Charge motions along the strand can be described by[10]

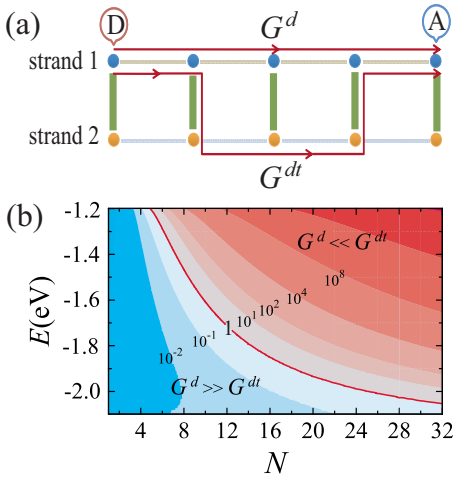

FIG. 1. (Color online) (a) The schematic picture presenting the direct and detour path for charge propagation in DNA duplex from the donor (D) to acceptor (A) site. The corresponding propagator (or the Green's functions) are defined in Eq. (6); (b) a preferential route diagram in the energy (E) vs the distance (N) plane, where the contour labels denote the ratio $|G^{dt}|/|G^d|$.

 ©2009 The American Physical Society

$$\mathcal{H}_{\parallel}^{(i)} = \sum_{\ell=1}^{N} \epsilon_i c_{i,\ell}^{\dagger} c_{i,\ell} - t_i \sum_{\langle \ell,m \rangle} (c_{i,\ell}^{\dagger} c_{i,m} + c_{i,m}^{\dagger} c_{i,\ell}), \tag{1}$$

with the strand index $i=1,2$, and $c_{i,\ell}(c_{i,\ell}^{\dagger})$ denoting the annihilation (creation) operator of an spinless electron at ℓth base of the strand i. The two strands can be coupled by the interstrand hopping as

$$\mathcal{H}_{\perp} = \sum_{i \neq j} \mathcal{H}_{\perp}^{(ij)} = -\sum_{i \neq j} \sum_{\ell=1}^{N} t_{\perp} c_{i,\ell}^{\dagger} c_{j,\ell} \tag{2}$$

so that the Hamiltonian for the molecule is given by $\mathcal{H}_{\mathrm{mol}} = \Sigma_{i=1}^{2} \mathcal{H}_{\parallel}^{(i)} + \mathcal{H}_{\perp}$. From the first-principles results, it is known that the almost decoupled poly(dX)-chain has highest occupied molecular orbital (HOMO) and lowest unoccupied molecular orbital (LUMO) band separated by a gap of a few eV.[11] Diagonalizing $\mathcal{H}_{\mathrm{mol}}$ with small $t_{\perp}$, we obtain the two energy bands,

$$E^{(i)}(k) \approx \epsilon_i - 2(-1)^i t_i \cos k, \quad i = 1,2. \tag{3}$$

Regarding, for example, the strand 1 as poly(dG) and strand 2 as poly(dC), ϵ_1 and ϵ_2 $(>\epsilon_1)$ determine the locations of the HOMO at guanine strand and the LUMO at cytosine strand, respectively, while t_i's determine the bandwidths. In our study, those band parameters are fixed from *ab initio* calculations.[11] For the donor-DNA-acceptor configuration of interest here [see Fig. 1(a)], the on-site energies of the end bases coupled to the charge reservoirs are modified as

$$\mathcal{H}_c = \sum_{s} (c_{i,1}^{\dagger} c_{i,1} + c_{j,N}^{\dagger} c_{j,N}). \tag{4}$$

The self-energy correction Σ_s is in general an energy-dependent complex number, but we discard its real part and simply set $\Sigma = -i\Gamma$. This can be justified by a weak coupling that makes negligible changes in the molecular energy levels and the energy dependence of the coupling strength, for which, we set $\Gamma = 0.005$ eV. Charge-transfer rate can be evaluated by $k = 2\pi/\hbar \int dE T(E) W(E - E_{\mathrm{in}}; \mu_{DA})$ with E_{in} being the energy of incident charge carrier and μ_{DA} being the chemical-potential difference between donor and acceptor. Here $W(E)$ is a weight function that selects the energy range and $T(E)$ is the probability for a charge carrier with energy E to transmit through the molecular bridge or the transmission. For small μ_{DA}, the system lies in the linear-response regime so that $k \approx (2\pi/\hbar)\mu_{DA} T(E_{\mathrm{in}})$, indicating that the transmission is a key factor to determine the characteristic behaviors of the charge transfer. It should also be mentioned that E_{in} for particle (hole) transfer is usually considered to be in the vicinity of HOMO (LUMO) bands of donor molecules. Meanwhile, in charge-transfer experiments, light irradiation is often used for creating charge carrier in charge-transfer experiments and would give rise to molecular excitations such as nonlinear lattice vibration. In this case, we need to consider inelastic-scattering processes, which would be done by microscopic modeling of the excitations and their coupling to charge carrier. In this work, we remain in the elastic-scattering picture but instead examine $T(E)$ for various carrier energies, which helps to infer the excitation effects. With the help of the Fisher-Lee relation, we can obtain the transmission by

$$T(E) = 4\Gamma^2 |G_{1N}|^2, \tag{5}$$

with G_{1N} being the component of the retarded Green's function $G = [(E + i0^+)I - \mathcal{H}_{\mathrm{mol}} - \mathcal{H}_c]^{-1}$. For our configuration where both acceptor and donor are located at the strand 1, we have $G_{1N} = [E - \mathcal{H}_{\parallel}^{(1)} - \mathcal{H}_c - \mathcal{H}_{\perp}^{(12)} \mathcal{G}^{(2)} \mathcal{H}_{\perp}^{(21)}]_{1N}^{-1}$, and by further using $\mathcal{H}_{\perp} \ll \mathcal{H}_{\parallel}$, $G_{1N} \approx G^d + G^{dt}$, where

$$G^d = [E - \mathcal{H}_{\parallel}^{(1)} - \mathcal{H}_c]_{1N}^{-1} \equiv \tilde{\mathcal{G}}_{1N}^{(1)},$$

$$G^{dt} = t_{\perp}^2 \sum_{\ell,m} \tilde{\mathcal{G}}_{1\ell}^{(1)} \mathcal{G}_{\ell m}^{(2)} \tilde{\mathcal{G}}_{mN}^{(1)}, \tag{6}$$

with $\mathcal{G}^{(i)} = [E - \mathcal{H}_{\parallel}^{(i)}]^{-1}$, and $\tilde{\mathcal{G}}^{(i)} = [E - \mathcal{H}_{\parallel}^{(i)} - \mathcal{H}_c]^{-1}$. The physical meanings of these Green's functions are clear from Fig. 1(a). While G^d represents a direct propagation without interstrand hopping, G^{dt} represents a "detour" propagation with partial route on the strand 2.

We can see that a key component in the propagators is the bare Green's function of the strand i, $\mathcal{G}^{(i)}$. Writing $\mathcal{H}_{\parallel}^{(1)}$ in the matrix representation, inversion can be readily done by $\mathcal{G}_{\ell m}^{(i)} = C_{m\ell}^{(i)} / \mathcal{D}_N^{(i)}$ with $\mathcal{D}_N^{(i)}$ and $C_{m\ell}^{(i)}$ being the determinant and the matrix cofactor of $[EI - \mathcal{H}_{\parallel}^{(i)}]$, respectively. The recursion relations between $\mathcal{D}_n$'s can be solved to yield $\mathcal{D}_n^{(i)}/t^n = S_{n+1}^{(i)}/S_1^{(i)}$ for even n and $\mathcal{D}_n^{(i)}/t^{n-1} = (E - \epsilon_i) S_{n+1}^{(i)}/S_2^{(i)}$ for odd n, where $S_n(\theta_i) = \sin(n\theta_i/2)$ and $\cos\theta_i = [(E-\epsilon_i)^2 - 2t_i^2]/2t_i^2$. Further algebra leads to the cofactor, $C_{ml}^{(i)} = (-1)^{l+m} \mathcal{D}_{S-1}^{(i)} \mathcal{D}_{N-L}^{(i)}$ with S and L denoting the smallest and the largest integers between l and m, respectively. Putting together, we obtain the bare Green's functions, especially those relevant to our investigation, as

$$t_i \mathcal{G}_{\ell=m}^{(i)} = \frac{(E - \epsilon_i) S_N(\theta_i)}{2\cos(\theta_i/2) S_{N+1}(\theta_i)}, \quad \text{for} \quad \ell = 1, N,$$

$$-t_i \mathcal{G}_{1N}^{(i)} = \frac{S_1(\theta_i)}{S_{N+1}(\theta_i)} \approx e^{-\beta_i N/2} \quad \text{for} \quad \beta_i \equiv \mathrm{Im}[\theta_i] \gg 1. \tag{7}$$

Note that the last line is valid also for $\mathcal{G}_{\ell m}^{(i)}$ if N is replaced with $|\ell - m + 1|$. Let us here note that θ_i can be real or imaginary, depending on the incident charge energy E. If E lies within the energy band of the strand i, that is, $0 < |E - \epsilon_i| < 2|t_i|$, θ_i is a real number. Otherwise, θ_i becomes imaginary, resulting in the exponential decay of the Green's functions.

Having in mind the energy dependence of $\mathcal{G}^{(i)}$, we first examine the case of $t_{\perp} = 0$. Since only one strand through which charges transmit is relevant here, for notation simplicity, let us drop the strand index and write the transmission of the decoupled strand allowed only by the direct path propagation as $T^d(E) = 4\Gamma^2 |G^d|^2$. Using the contact Hamiltonian $\mathcal{H}_c$ given by Eq. (4) with $i=j$, we obtain $\tilde{\mathcal{G}}_{1N} = \mathcal{G}_{1N}/\det M$, where $M_{\ell m} = \delta_{\ell m} - i\Gamma \mathcal{G}_{\ell m}$ with $\ell, m = 1, N$. After some manipulation, we arrive at

$$G^d = -\frac{1}{t}\frac{S_1}{\gamma^2 S_{N-1} - S_{N+1} + 2i\gamma S_N}, \tag{8}$$

with $\gamma=\Gamma/t$. Let us remind the fact that S's here depend on E through θ. When E coincides with the energy levels of the strand $[E=E^{(i)}(k)$ given by Eq. (3)], we have $\theta/2=k$ with $0 \le k \le \pi/2$. On the other hand, for E lying in the band-gap region, θ is an imaginary number. Once we have reflected these energy dependence of θ in G^d given by Eq. (8), we obtain the resulting transmission which shows various types of decay as

$$T^d = \begin{cases} 1, & E = E^{(i)}(k), \quad k \approx n\pi/(N+1) \\ 4\gamma^2(1+\gamma^2)^{-2}, & E = \epsilon_i \\ 4\gamma^2 e^{-\beta N}, & E \gg E^{(1)}, \quad E \ll E^{(2)}, \end{cases} \tag{9}$$

with n being integers. In the first line, we recover the familiar resonance transmission inside the energy band. The transmission for the band edge is given by the fractional number, as the second line reads. The exponential decays are also reported in the previous studies.[3,4,6] Yet, it is remarkable here that those various decay types could be found in a single framework of quantum transport theory. For the tunneling through the band gap, the corresponding transmission is given by the last line of Eq. (9), which decays exponentially with N. The decay scale, the so-called β value, is given by $\beta=\ln[|\xi|+\sqrt{\xi^2-1}] \approx \ln|2\xi| \approx 2\ln[(E-\epsilon)/t]$ with $\xi=-1+(E-\epsilon)^2/2t^2$. Interestingly, it is identical to the decay scale obtained in the McConnell[12] model.

We now switch on the coupling between the two strands. For a specific example, consider a poly(dG)-poly(dC) with both donor and acceptor located in poly(dG) (strand 1). Let us first discuss our numerical results presented in Fig. 2. When E lies within or near the energy levels of poly(dG), the detour propagation is strongly suppressed because $\mathcal{G}^{(2)}_{\ell m} \sim e^{-|\ell-m|\beta_2}$ with $\beta_2 \gg 1$. For the case, we expect $T(E) \approx 4\gamma^2|G^d|^2$, and hence $T(E) \approx T^d$. This is indeed so, as the lower panel of Fig. 2 shows that the analytic results (lines) given by Eq. (9) are perfectly consistent with the numerical data (points). On the other hand, when E is close to the energy levels of poly(dC), the propagation along the G chain in turn rapidly decays with distance so that G^d becomes negligible and the detour propagation $G^{dt} \approx (t_\perp/t_1)^2 \mathcal{G}^{(2)}_{1N}$ would make a major contribution. Since for the process, poly(dG) is effectively absent, the length dependence of the corresponding transmission would remain the same as T^d apart from its magnitude roughly $t_\perp^4$ times smaller, as the lower peaks indicate in Fig. 2(a). For the intermediate energy range such as $\epsilon_G+2t_G<E<\epsilon_C-2t_C$, a question naturally arises which of the direct and the detour propagation would be dominant. This can be answered by examining $|G^{dt}|/|G^d|$. Using the bare Green's functions for both strands exponentially decay in the energy regions [see Eq. (7) together with its corresponding discussion], we evaluate Eq. (6) to reach

$$\frac{|G^{dt}|}{|G^d|} = \Lambda \frac{x^{N/2}-1}{(x-1)^2}, \tag{10}$$

with $\Lambda \equiv t_\perp^2 e^{-\beta_2}/t_1 t_2$ and $x \equiv e^{\beta_1-\beta_2}$. A given carrier energy fixes the decay scales and hence x. In Fig. 3(a), we plot Eq. (10) for various values of E, for which the effective pathway of charge transfer is determined by N. For our discussion, let us define the crossover length by $|G^{dt}|/|G^d|_{N=N_c}=1$ for a given E; for example, $N_c \approx 4$ for $E=-1.192$ eV. This allows us to conclude that for $N>N_c$, charge transfer occurs mainly via detour propagation, while for $N<N_c$, direct propagation prevails. Although Eq. (10) cannot be solved to express N_c in terms of the energy, it is worthwhile examining the limiting cases. Considering the case of $x \gg 1$, where the direct path has far shorter decay scale, we have $N_c \approx 4-2\ln\Lambda/\ln x$. For the case, N_c is small so that for a relatively longer distance transfer, the detour path along the slowly decaying complementary strand is advantageous. Interestingly, however, we see that there exists a lower bound of N_c such as $N_c \ge 4$. This indicates that for a charge transfer over a distance shorter than four base pairs, charges always prefer the direct path to the detour despite the slow decay of the latter.

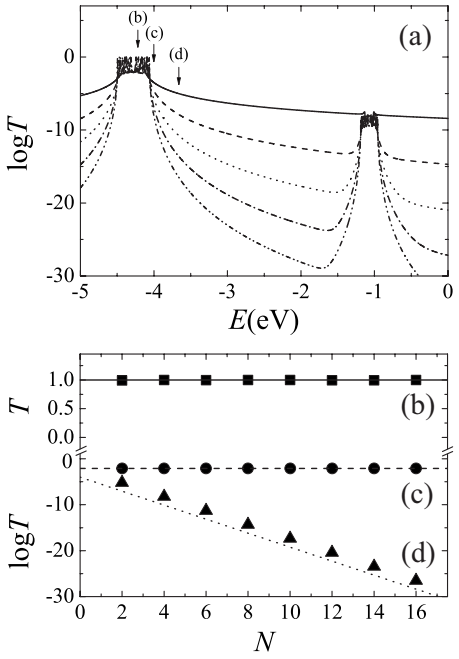

FIG. 2. (a) The dimensionless charge-transfer rate of poly(dG)-poly(dC) for the various molecule lengths (2, 4, 6, 8, and 10 in descending order). According to the energy location, T displays different length dependence. We sample the energy values indicated by the arrows and display the corresponding length dependence in the lower panel where the points obtained by numerical calculation and the lines from Eq. (9). The parameters for numerical computations are $\epsilon_G=-4.278$ eV, $t_G=0.114$ eV, $\epsilon_C=-1.072$ eV, $t_C=0.060$ eV, and $t_\perp=0.034$ eV, which will be used throughout this work.

Let us discuss a nontrivial consequence of the crossover distance on the length dependence of the transfer rate. We numerically evaluate the transmission for the E values in Fig. 3(a) for comparison. As shown in Fig. 3(b) (see, e.g., $E=-1.192$ eV), the decay scales abruptly changes at $N_c \approx 4$, well correspondent with the analytic result. To observe the decay scale crossover, on the other hand, N_c should be not so large for T experimentally appreciable. This crucially depends on the charge-carrier energy. When $x \approx 1 (E \approx -2.177$ eV) where the two strands has comparable decay

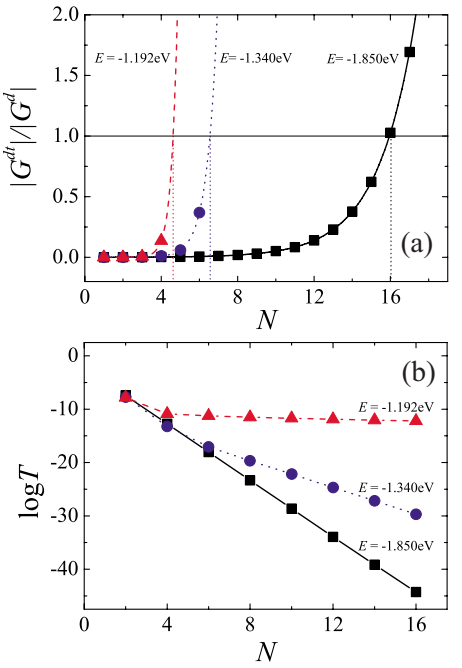

FIG. 3. (Color online) (a) $|G^{dt}|/|G^{d}|$ vs the length of poly(dG)-poly(dC) for various values of x, where the crossover length is determined by $|G^{dt}|/|G^{d}|=1$ for a given x and (b) the length dependence of the charge-transfer rate that undergoes a decay scale crossover at N_c.

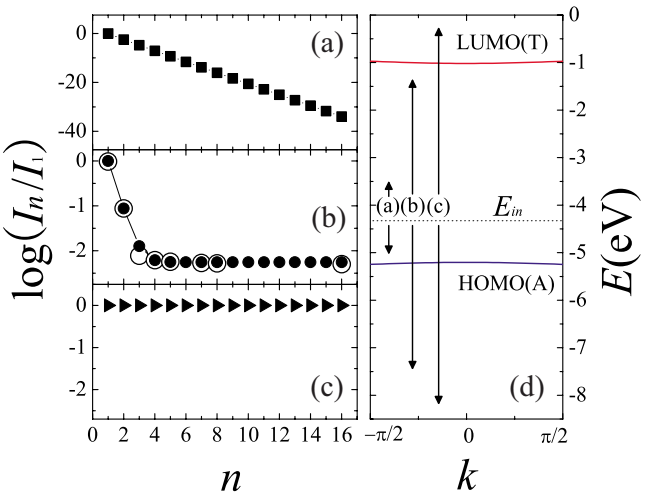

FIG. 4. (Color online) Charge-transfer rates through T_n bridge for (a) $w=0.70$ eV, (b) $w=3.23$ eV, and (c) $w=4.00$ eV, displaying the exponential decay, the crossover, and the length independence, respectively. The energy ranges in the cases are denoted in (d) which is the energy diagram reproduced by Eq. (3) with the tight-binding parameters (in the unit of eV) $\epsilon_A=-5.245$, $\epsilon_T=-0.972$, $t_A=0.021$, $t_T=0.023$, and $t_\perp=0.030$.

scales, we obtain $N_c^2 \approx 8\Lambda^{-1}$, which can be large when $\Lambda \ll 1$. For the case, the decay scale crossover is unlikely to observe—but instead—the transfer displays the single scale such as many of experiments.[5,13] In fact, the crossover between the fast and slow decay was experimentally observed in a DNA of base sequence $G(T)_N GGG$.[9] On the other hand, we find that the phenomenon is not specific to the T bridge but can also occur in a guanine bridge; note that the crossover behavior presented in Fig. 3(b) is obtained for $G(G)_N GGG$. Let us now demonstrate that the crossover observed in the charge-transfer rate of $G(T)_N GGG$ (Ref. 9) has the same origin. To do so, we set the energy of incident charge to be in the vicinity of HOMO of gua base[11] and take the weight function to determine the energy window contributing to the charge transfer, as $W(E)=1$ for $E-E_{\text{in}} \in [-w, w]$ and $W(E)=0$ otherwise. We consider three cases according to which strand accommodates the molecular orbital inside the energy window: (a) none, (b) adenine, and (c) thymine [see Fig. 4(d) showing the molecular orbitals and the arrows therein indicating the energy window widths for the three cases]. In the case of (a), charges tunnel through the band gap and hence the transfer rate exhibits the exponential decay, as shown in Fig. 4(a). Increasing w to include HOMO of adenine, the crossover from fast to slow decay occurs [see Fig. 4(b)] such as the experiment and as found in the transmission of guanine bridge. Increasing w further to be in the case (c), charges travel via the direct path along the thymine strand providing resonance states, resulting in the length-independent transfer. It should be noted that the chemical-potential difference between donor and acceptor μ_{DA} determines the energy window width and therefore the decay behavior. In the experiment,[9] no direct clue for the value of μ_{DA} is available. On the other hand, our results interpret μ_{DA} to be in the case (b) and also suggest future experimental test if the variety of the length dependence of transfer rate is realizable by controlling μ_{DA}.

In summary, we have studied the charge transmission probability analytically and numerically. We have obtained various length dependences for the transmission probability according to the incident charge energy: the length-independent resonant transmission within the energy band and the exponential decay inside the band-gap region. Interestingly, in the band-gap region, the decay scale crossover is found to occur as a consequence of the competition between the direct path and the detour path, well explaining the experimental observation. Although not presented here, we have also considered environmental fluctuations by introducing a randomness in the hopping integral caused by thermally agitated random deformations of molecular structure. We have found that the length-dependence behaviors are preserved even in the presence of fairly strong randomness, except the length-independent resonance transmission which for finite randomness decays exponentially, signifying the localization effects. We have also evaluated the localization lengths for various randomness strengths and have confirmed that they are much longer than the tunneling length. This well explains our finding that the decay behavior in the tunneling regime is robust against the structural randomness.

This work was supported by the Korea Science and Engineering Foundation (Grant No. R01-2007-000-20084-0).

[1] D. D. Eley and D. I. Spivey, Trans. Faraday Soc. **58**, 411 (1962).
[2] M. Ratner, Nature (London) **397**, 480 (1999); R. G. Endres, D. L. Cox, and R. R. P. Singh, Rev. Mod. Phys. **76**, 195 (2004) and references therein.
[3] R. A. Marcus and N. Sutin, Biochim. Biophys. Acta **811**, 265 (1985).
[4] J. Jortner, M. Bixon, T. Langenbacher, and M. E. Michel-Beyerle, Proc. Natl. Acad. Sci. U.S.A. **95**, 12759 (1998).
[5] C. J. Murphy, M. R. Arkin, Y. Jenkins, N. D. Ghatlia, G. H. Bossmann, N. J. Turro, and J. K. Barton, Science **262**, 1025 (1993); E. Meggers, M. E. Michel-Beyerle, and B. J. Giese, J. Am. Chem. Soc. **120**, 12950 (1998); S. O. Kelley and J. K. Barton, Science **283**, 375 (1999); F. D. Lewis, J. Liu, W. Weigel, W. Rettig, I. V. Kurnikov, and D. N. Beratan, Proc. Natl. Acad. Sci. U.S.A. **99**, 12536 (2002).
[6] M. Bixon, B. Giese, S. Wessely, T. Landenbacher, M. E. Mechel-Beyerle, and J. Jortner, Proc. Natl. Acad. Sci. U.S.A. **96**, 11713 (1999).
[7] *Long-Range Charge Transfer in DNA*, edited by G. B. Schuster (Springer-Verlag, Berlin, 2004) and references therein.
[8] D. S. Fisher and P. A. Lee, Phys. Rev. B **23**, 6851 (1981); S. Datta, *Electronic Transport in Mesoscopic Systems* (Cambridge University Press, Cambridge, 1999).
[9] B. Giese, J. Amaudrut, A. Kölher, M. Spormann, and S. Wessely, Nature (London) **412**, 318 (2001).
[10] J. Yi and B. J. Kim, Phys. Rev. B **75**, 035111 (2007).
[11] H. Mehrez and M. P. Anantram, Phys. Rev. B **71**, 115405 (2005).
[12] H. M. McConnell, J. Chem. Phys. **35**, 508 (1961).
[13] P. T. Henderson, D. Jones, G. Hampikian, Y. Kan, and G. B. Schuster, Proc. Natl. Acad. Sci. U.S.A. **96**, 8353 (1999).